

## Single Case

---

# Low-Vacuum Scanning Electron Microscopy to Assess Histopathological Resolution of Class V Lupus Nephritis: A Case Report

Maria Yoshida<sup>a</sup> Shuma Hirashio<sup>a</sup> Toshiki Doi<sup>a</sup> Yukinari Masuda<sup>a</sup>  
Akira Shimizu<sup>b</sup> Takao Masaki<sup>a</sup>

<sup>a</sup>Department of Nephrology, Hiroshima University Hospital, Hiroshima, Japan;

<sup>b</sup>Department of Analytic Human Pathology, Nippon Medical School, Tokyo, Japan

## Keywords

Immunofluorescence staining · Immunoglobulin deposits · Low-vacuum scanning electron microscopy · Lupus nephritis · Systemic lupus erythematosus

## Abstract

Lupus nephritis (LN) is most frequently associated with poor outcomes in patients with systemic lupus erythematosus (SLE). LN manifests as histopathological changes in the kidney caused by immune complex formation and deposition. In particular, immunoglobulin G (IgG) deposits are frequently observed by immunofluorescence staining, which helps to establish the diagnosis of LN. In this case report, we describe a 57-year-old woman with SLE who had been undergoing treatment on an outpatient basis for 11 years. Her first and second renal biopsies revealed class V LN with a coarsely granular pattern of IgG deposition in the peripheral capillary walls. However, her third renal biopsy showed no IgG deposition, which indicated

histopathological resolution of her class V LN. We used low-vacuum scanning electron microscopy (LV-SEM) to examine the three-dimensional structural alterations in her glomerular basement membranes. In this report, we describe findings that indicated resorption of epithelial deposits, that is, resolution of LN. The results of repeated kidney biopsies confirmed by LV-SEM suggested the possibility of a state unrelated to LN.

© 2021 The Author(s)  
Published by S. Karger AG, Basel

## Introduction

Systemic lupus erythematosus (SLE) is a multiorgan, systemic autoimmune disease with clinical and serological heterogeneity [1]. Lupus nephritis (LN) is one of the most common and devastating manifestations of SLE. In approximately 50% of affected patients, SLE results in LN [2]. Although the overall mortality of patients with SLE has decreased remarkably in recent decades, renal disease remains the leading cause of death in these patients [3]. LN has histopathological diversity and is explained by immune complex deposition [4, 5]. Renal biopsy allows for evaluation of LN activity and determination of therapy based on histological features. Although individual patterns of immunofluorescence (IF) staining are highly variable, some general characteristics are applicable to all classes [4]. In more than 90% of patients with SLE, IF staining of the peripheral capillary wall or mesangial areas is seen microscopically. In particular, immunoglobulin G (IgG) deposits are observed using IF staining in almost every patient with LN [4, 6]. In most cases of LN, immune complexes in blood plasma are deposited on glomeruli, which can be seen using light microscopy (LM), IF, and transmission electron microscopy (TEM) [7].

In the present case, we performed three renal biopsies in 9 years. The first and second renal biopsies revealed IgG deposits in the peripheral capillary walls; however, the third renal biopsy showed no IgG deposits. Conventional renal biopsy paraffin sections stained with periodic acid methenamine silver (PAM) can be directly observed using low-vacuum scanning electron microscopy (LV-SEM). In conventional electron microscopy, only a small area can be viewed; however, LV-SEM enables scanning over broad areas of the specimen and in three dimensions under high magnification [8, 9]. We considered that evaluation using LV-SEM might be useful for the histopathological assessment of renal glomerular basement membrane (GBM) alterations. We therefore evaluated the two sides of the GBM using LV-SEM and examined the washout phenomenon of the membranous form of LN. We herein highlight the histopathological findings of this case.

## Case Presentation

### *Clinical Information*

A 57-year-old woman had presented with Raynaud's phenomenon and fever of unknown etiology at the age of 48 years. Laboratory analysis showed positive anti-nuclear autoantibody and renal insufficiency with proteinuria (1.33 g/g Cr). The titer of anti-double-stranded DNA

autoantibody was slightly elevated (3.1 IU/mL). She was diagnosed with SLE in accordance with the Systemic Lupus International Collaborating Clinics criteria [10]. The patient's first renal biopsy was undertaken at this time. Examination of the biopsy specimen led to a diagnosis of class V LN in accordance with the World Health Organization classification [9]. According to this diagnosis, she was treated with oral prednisolone, and tacrolimus was added at the age of 49 years. These treatments were successful, and the urine protein level decreased remarkably 4 years after treatment was started (to around 0.3–0.4 g/g Cr). At the age of 53 years, she was treated with dose-reduced tacrolimus because the effectiveness of these treatments had been confirmed. Despite the slow improvement in her renal function, the severity of her proteinuria gradually increased during the 4 years since the first biopsy. We suspected recurrence, and she therefore underwent a second biopsy at the age of 54 years. This repeat biopsy also revealed class V LN. Based on these findings, mycophenolate mofetil at 1,250 mg/day was added to the treatment regimen.

At the age of 57 years, laboratory studies revealed low SLE activity with a normal complete blood count, normal complement protein levels, and an anti-double-stranded DNA antibody titer of 5.8 IU/mL; however, proteinuria was present (>2 g/g Cr) (Table 1). Therefore, she underwent a third renal biopsy at the age of 57 years. At this time, the patient's clinical course and immunological investigation indicated no progression of SLE. Because the pathological findings indicated negative conversion of IgG, we considered that the activity of LN had been lost. These pathological results could explain the decreased SLE activity, and the class V LN was presumed to have resolved.

The patient was subsequently treated with antihypertensive drugs with a focus on angiotensin II receptor antagonists. Following treatment, her proteinuria decreased to 0.5 g/g Cr.

### *Renal Biopsies*

The patient's first renal biopsy was performed at the age of 48 years. Histopathological examination using LM revealed several foamy formations and a generalized diffuse thickening of the GBM, which manifested as prominent spikes on PAM silver staining (Fig. 1a1). On IF staining, coarsely granular deposits of IgG, C3, and C1q were evident in the capillary walls (Fig. 1a2). TEM revealed abundant subepithelial deposits lining all capillary loops (Fig. 1a3). The patient was diagnosed with LN class V according to the International Society of Nephrology/Renal Pathology Society classification.

The second biopsy at the age of 54 years revealed reduced spike formation and a bubbly appearance (stippling) under LM examination (Fig. 1b1). IF staining showed similar findings; coarsely granular deposits of IgG, C3, and C1q were evident in the capillary basement membrane (Fig. 1b2). On TEM, smaller electron-dense deposits than in the first renal biopsy suggested a resorptive process (Fig. 1b3). A well-developed GBM reaction surrounded the deposits with overlying foot process effacement. These findings also indicated type V LN.

The third biopsy at the age of 57 years revealed advanced glomerulosclerosis (5/25 glomeruli), and PAM silver staining exhibited a primarily bubbly appearance and dome patterns; the spikes had almost disappeared on LM examination (Fig. 1c1). Conversely, the IF findings showed a scattered distribution of the IgG deposits with negative C3 and C1q (Fig. 1c2). TEM also revealed a marked decrease in the electron density of the deposits that had been clearly

seen in the previous two biopsies. Instead, GBM thickening and wrinkling were seen (Fig. 1c3). We doubted that the results of TEM and IF therefore differed from those of LM. Another remarkable finding on LM was arteriolar hyalinosis, which could be explained as arteriolopathy caused by calcineurin inhibitors. No evidence of calcineurin inhibitor toxicity such as striped interstitial fibrosis or tubular atrophy was observed. Tubular and interstitial lesions were attributed to the effect of renal sclerosis because of hypertension. The increase in urinary protein excretion could be explained by severe arterial sclerosis and calcineurin inhibitor-induced arteriolopathy rather than exacerbation of LN.

C4d is described as a byproduct of activation of the classical and lectin pathways. Because C4d acts as a positive marker for an immune complex-mediated mechanism in glomerular nephritis, C4d staining can be helpful in revealing immune complex deposition [11]. Unfortunately, we could not examine the C4d properties of the deposits using frozen sections because of a lack of additional tissue remaining in the block. Therefore, to confirm that LN was not the main cause of the clinical proteinuria, we investigated the GBM using a different method.

For further evaluation, we observed the GBM in all three biopsy specimens using LV-SEM (Hitachi Tabletop microscope TM4000; Hitachi High-Technologies Corp., Tokyo, Japan). In the first renal biopsy at the age of 48 years, LV-SEM of glomeruli retrieved from formalin-fixed paraffin-embedded tissue (PAM stain) revealed extensive and numerous subepithelial holes where deposits were thought to have been present. Additionally, well-developed GBM material formed spikes around the holes (Fig. 2a1). However, these holes were not found on the glomerular capillary luminal side (Fig. 2a2). This finding corresponded to Ehrenreich-Churg stage II membranous nephropathy (MN). The second renal biopsy at the age of 54 years showed a well-developed GBM reaction surrounding the holes where deposits might have been present; this finding was equivalent to Ehrenreich-Churg stage III MN (Fig. 2b1). Epithelium had formed and covered holes found in the first renal biopsy tissue, and it was difficult to see holes when looking down from the subepithelial side (Fig. 2b1). The GBM of the glomerular capillary lumina was almost covered by basement membrane material, and holes were still only partially open (Fig. 2b2). The third renal biopsy at the age of 57 years exhibited epithelium covered by newly formed GBM material, with openings in the GBM inward toward the glomerular capillary lumen (Fig. 2c1, c2). We speculated that the holes in the glomerular capillary luminal side might emerge when immune complex deposits in the GBM wash out.

In studying the third renal biopsy specimen, we also drew a comparison between the IF findings of the scattered distribution of the deposits and the LV-SEM findings. We stained frozen sections for IF with PAM and examined them with LV-SEM. We compared and observed the same glomeruli (Fig. 3). No IgG staining was confirmed using IF, which suggested that no deposits were present in the GBM (Fig. 3a). However, many cavities were confirmed using LV-SEM (Fig. 3b). Therefore, it was considered that no deposit was present in the many holes, and it was presumed that washout of the immune complex deposits occurred in the membranous LN. Overall, further observation of the GBM with LV-SEM confirmed resolution of class V LN. This case was similar to stage IV MN according to the Ehrenreich-Churg staging criteria.

A case report by Nonaka et al. [12] described the conventional TEM assessment of subepithelial deposits in a patient with mild membranous LN. However, few cases of LN evaluated using LV-SEM in which the loss of immune complex deposits was discovered have been

reported. Clinicians emphasize IgG deposition in the diagnosis of LN. Many clinicians tend to consider that LN is highly unlikely if IgG is negative using IF examination. In the present case, however, the diagnosis of LN was confirmed in the first and second renal biopsies.

This is our first experience of a case in which the pathological findings were presumed to indicate a state of resolution of class V LN, and we thought that this was a highly contradictory finding. We had doubts regarding whether the histopathological findings of LN disappear (as in common MN) as the disease activity of SLE decreases.

## Discussion/Conclusion

In the present study, we found that membranous LN diminished or resolved over the course of the three renal biopsies. To help clarify this process, we evaluated the patient's kidney biopsy tissue using LV-SEM, which allows for observation of both sides of the GBM. By studying the three-dimensional structure of the GBM using LV-SEM, we confirmed the formation of holes on the glomerular capillary luminal side. From these findings, we suspected that the same pathology of the membrane washout phenomenon that occurs in MN occurred in our patient with LN.

LV-SEM sometimes outperforms the conventional technique, TEM. TEM is the superior technique for investigating cross-sectional images of various components in glomeruli; however, performing three-dimensional and whole/wide observations using ultrathin sections is difficult because of the limitation of the observable size. LV-SEM can be used to evaluate the three-dimensional ultrastructural changes of the glomerular extracellular matrices in the same specimen used for LM. It thus provides more detailed three-dimensional information [8, 9]. Therefore, to review the morphological alterations of the glomeruli in a three-dimensional, broad area, we examined the LM slides of the renal biopsy specimens using LV-SEM.

LV-SEM examination of the first biopsy revealed many openings or holes in the subepithelium, consistent with the LM, IF, and TEM findings. The second renal biopsy showed a well-developed GBM reaction surrounding the openings or holes with overlying foot process effacement. These LV-SEM results were almost identical to those of TEM. The third renal biopsy showed openings on the thickened GBM inward toward the glomerular capillary lumina and loss of the electron density of the deposits in TEM. We confirmed the findings of some openings or holes in the GBM on the luminal side of the vessel using LV-SEM. Thus, we suspected that the deposits were washed out through these holes. In other words, the findings we confirmed using LV-SEM might result from washout of the immune complexes (only the cavity remained after washout). This concept allows for the possibility of finding IgG positivity on IF, which can be said to be an essential marker of LN. IgG was negative using IF in the tissue from the third renal biopsy in this patient.

Furthermore, it is possible that LV-SEM might be useful for monitoring disease, in contrast to interpreting potentially challenging serological results. An example is M-type phospholipase A2 receptor (PLA2R)-negative MN. PLA2R-negative secondary MN is generally characterized by the irregular distribution and size of subepithelial deposits and the presence of irregular subendothelial and mesangial deposits in glomeruli. We believe that there may be

some difference in the GBM of PRA2R-positive or -negative MN evaluated in detail using LV-SEM.

The Ehrenreich-Churg classification divides MN into four pathological stages according to the state of immune complex deposition and change in the GBM [13]. Stage IV MN is characterized by loss of the electron density of the deposits, transition to a “washout” state, and development of electron-lucent zones within an irregularly thickened GBM [13]. Furthermore, the GBM recovers to an almost normal morphology in stage V MN [14]. The GBM returns to its normal form without deposition or thickening in the state of washed-out MN. In the present case, however, LM did not show findings consistent with normalization of the GBM morphology, similar to the washout image seen in stage IV or V MN, and changes such as thickening and spike formation persisted. However, IgG and C3 deposits cannot be seen using IF staining. TEM also exhibited few deposits. This series of pathophysiological findings has been confirmed by observations on resolving glomerulopathy in serial allograft biopsies [15].

Based on these results, we postulated a pathological process beginning with LN that caused deposition of immune complexes on the GBM. A decrease in LN activity then led to loss of these deposits as the disease progressed to a state of stage V MN washout, which results in a bubbly appearance. That is, despite resolution of LN, LM showed a remarkable change in the GBM. When LM shows noticeable changes in the GBM and specific clinical findings are present (excessive urinary protein), clinicians will usually think that the cause is LN.

The opening on the GBM is normally covered by vascular endothelium. However, in MN, complement complexes might injure the GBM by inducing the production of reactive oxygen species, thus altering the membrane structure [16]. At that time, a large proportion of the immune complex might have passed through the GBM from the glomerular capillary luminal side toward the epithelial side and nephrosis developed. We suspected that in the present case, this backward event (from the epithelial side toward the glomerular capillary luminal side) could have occurred during the LN washout phase. In other words, we suspected the possibility that these holes observed on the glomerular capillary luminal side were formed when the immune complexes were washed out.

In conclusion, our patient exhibited a loss of LN activity and a change to a state of resolution of class V LN. Renal biopsy revealed negative conversion of IgG on IF, and spikes and domes were present in the GBM on LM. We believe that the evaluation of three-dimensional structural alterations in GBM using LV-SEM might be a useful approach for assessing variation in renal biopsies over time.

## Acknowledgments

We thank Angela Morben, DVM, ELS, and Andrea Baird, MD, from Edanz Group (<https://en-author-services.edanzgroup.com/>), for editing drafts of the manuscript.

## Statement of Ethics

This study was conducted according to the guidelines laid down in the World Medical Association Declaration of Helsinki. Informed consent was obtained from the patient described in this case report, and the consent allowed their data to be stored, as required by the Hiroshima University Hospital. Written consent to publish this information was obtained from the patient (images and publication).

## Conflict of Interest Statement

The authors have no conflicts of interest to declare.

## Funding Sources

This study was not funded by any third party.

## Author Contributions

M.Y., S.H., and T.D. contributed to the data collection. S.H. and T.M. designed the research. Y.M. and A.S. evaluated the pathological tissue. M.Y. and S.H. performed the primary manuscript preparation. M.Y., S.H., T.D., and T.M. wrote the paper. T.M. has primary responsibility for the final content. M.Y., S.H., T.D., Y.M., and A.S. reviewed the paper and revised it critically. All authors read and approved the final manuscript.

## References

- 1 Yu C, Gershwin ME, Chang C. Diagnostic criteria for systemic lupus erythematosus: a critical review. *J Autoimmun.* 2014 Feb-Mar;48-49:10–3.
- 2 Haładaj E, Cervera R. Do we still need renal biopsy in lupus nephritis? *Reumatologia.* 2016;54(2):61–6.
- 3 Giannico G, Fogo AB. Lupus nephritis: is the kidney biopsy currently necessary in the management of lupus nephritis? *Clin J Am Soc Nephrol.* 2013 Jan;8(1):138–45.
- 4 D'Agati VD, Stokes MB. Renal Disease in Systemic Lupus Erythematosus, Mixed Connective Tissue Disease, Sjögren's syndrome, and Rheumatoid Arthritis. In: Jennette JC, D'Agati VD, Olson JL, Silva FG, editors. *Heptinstall's Pathology of the Kidney.* 7th ed. Philadelphia: Wolters Kluwer; 2014. pp. 559–656.
- 5 Lorenz G, Anders HJ. Neutrophils, Dendritic Cells, Toll-Like Receptors, and Interferon- $\alpha$  in Lupus Nephritis. *Semin Nephrol.* 2015 Sep;35(5):410–26.
- 6 Méry JP, Morel-Maroger L, Boelaert J. Immunoglobulin and complement deposits in lupus glomerulonephritis. *Proc Eur Dial Transplant Assoc.* 1975;11:506–11.
- 7 Behara VY, Whittier WL, Korbet SM, Schwartz MM, Martens M, Lewis EJ. Pathogenetic features of severe segmental lupus nephritis. *Nephrol Dial Transplant.* 2010 Jan;25(1):153–9.
- 8 Inaga S, Kato M, Hirashima S, Munemura C, Okada S, Kameie T, et al. Rapid three-dimensional analysis of renal biopsy sections by low vacuum scanning electron microscopy. *Arch Histol Cytol.* 2010;73(3):113–25.

- 9 Okada S, Inaga S, Kawaba Y, Hanada T, Hayashi A, Nakane H, et al. A novel approach to the histological diagnosis of pediatric nephrotic syndrome by low vacuum scanning electron microscopy. *Biomed Res.* 2014;35(4):227–36.
- 10 Petri M, Orbai AM, Alarcón GS, Gordon C, Merrill JT, Fortin PR, et al. Derivation and validation of the Systemic Lupus International Collaborating Clinics classification criteria for systemic lupus erythematosus. *Arthritis Rheum.* 2012 Aug;64(8):2677–86.
- 11 Sethi S, Nasr SH, De Vriese AS, Fervenza FC. C4d as a Diagnostic Tool in Proliferative GN. *J Am Soc Nephrol.* 2015 Nov;26(11):2852–9.
- 12 Nonaka K, Ubara Y, Suwabe T, Takaichi K, Oohashi K. Intractable membranous lupus nephritis showing selective improvement of subepithelial deposits with tacrolimus therapy: a case report. *Clin Nephrol.* 2013 Aug;80(2):140–5.
- 13 Ehrenreich T, Churg J. Pathology of membranous nephropathy. *Pathol Annu.* 1968;3:145–86.
- 14 Gärtner HV, Watanabe T, Ott V, Adam A, Bohle A, Edel HH, et al. Correlations between morphologic and clinical features in idiopathic perimembranous glomerulonephritis. A study on 403 renal biopsies of 367 patients. *Curr Top Pathol.* 1977;65:1–29.
- 15 Mirza MK, Kim L, Kadambi PV, Chang A, Meehan SM. Membranous nephropathy transplanted in the donor kidney: observations of resolving glomerulopathy in serial allograft biopsies. *Nephrol Dial Transplant.* 2014 Dec;29(12):2343–7.
- 16 Starzyńska-Kubicka A, Perkowska-Ptasińska A, Górnicka B. Membranous glomerulonephritis - a common, unspecific pattern of glomerular injury. *Pol J Pathol.* 2018;69(3):209–18.

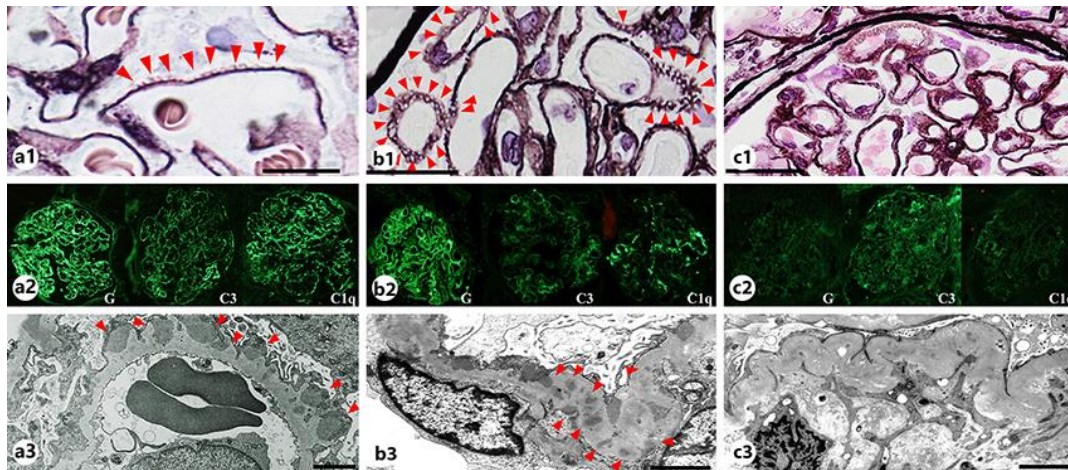


**Fig. 1.** Renal biopsy findings. **a** First renal biopsy. **a1** LM revealed that the basement membrane was thickened and exhibited mainly spikes (red arrowheads) (PAM stain). Scale bar, 25  $\mu$ m. **a2** IF staining demonstrated coarsely granular deposits of IgG, C3, and C1q in the capillary walls (IF microscopy, IgG, C3, C1q;  $\times 200$ ). **a3** TEM showed abundant subepithelial deposits. The pattern was equivalent to Ehrenreich-Churg stage II MN. Scale bar, 2  $\mu$ m (TEM). **b** Second renal biopsy. **b1** The basement membrane showed a global increase in thickening and a bubbly appearance on LM (red arrowheads). This appearance was comparable with Ehrenreich-Churg stage III MN (PAM stain). Scale bar, 50  $\mu$ m. **b2** IF exhibited coarsely granular deposits of IgG, C3, and C1q in the capillary basement membrane, as in the previous examination (IF microscopy, IgG, C3, C1q;  $\times 200$ ). **b3** TEM examination showed that the dense deposits were smaller and had been partly resorbed. A well-developed basement membrane reaction surrounded the deposits with overlying foot process effacement. Scale bar, 2  $\mu$ m (TEM). **c** Third renal biopsy. **c1** The basement membrane was thickened and exhibited a general meandering-like wrinkling pattern as seen on LM. The bubbly appearance was the same as in the second biopsies (PAM stain). Scale bar, 50  $\mu$ m. **c2** IF showed almost negative conversion of IgG and negative C3 and C1q (IF microscopy, IgG, C3, C1q;  $\times 200$ ). **c3** On TEM, the basement membrane showed global thickening, wrinkling, and podocyte foot process effacement. The electron density of the deposits was unclear. Scale bar, 2  $\mu$ m (TEM). C, complement; IF, immunofluorescence; IgG, immunoglobulin G; LM, light microscopy; MN, membranous nephropathy; PAM, periodic acid methenamine silver; TEM, transmission electron microscopy.

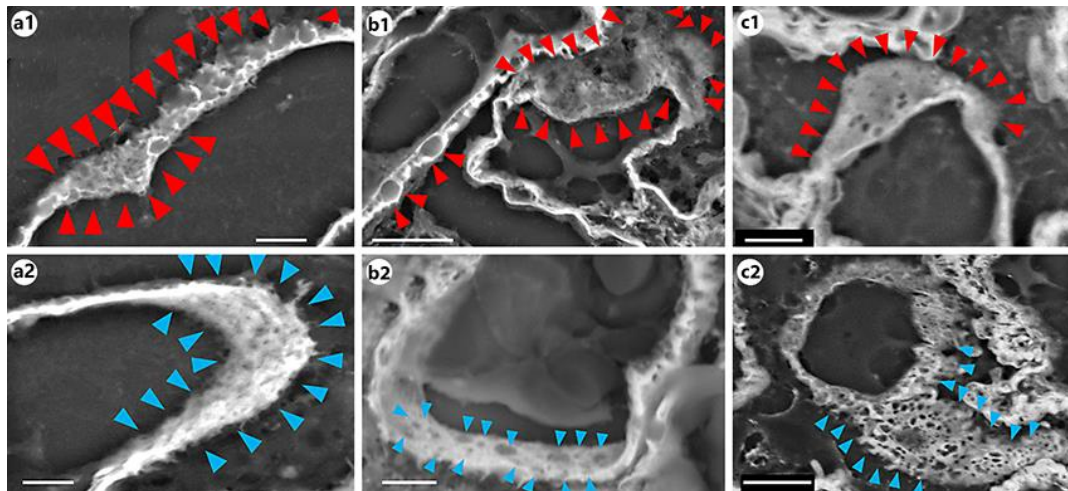


**Fig. 2.** Renal biopsy findings using LV-SEM. **a** First renal biopsy. **a1** An image from the epithelial side of the GBM. Basement membrane material accumulated between many holes (deposit-like appearance) and projected into the urinary space as “spikes” (red arrowheads). The holes were not covered with basement membrane. Scale bar, 2.5  $\mu\text{m}$ . **a2** An image from the glomerular capillary lumina. The GBM of the glomerular capillary luminal side was covered by the material of the basement membrane, and no opening was seen (blue arrowheads). Scale bar, 2.5  $\mu\text{m}$ . **b** Second renal biopsy. **b1** An image from the epithelial side of the GBM. Intramembranous holes were observed. These holes (deposit-like appearance) were surrounded by well-developed basement membrane material (red arrowheads). In the subepithelium of the GBM, basement membrane material was newly formed on the holes, and the holes seen in **a1** could not be confirmed from the epithelium side view. Scale bar, 5  $\mu\text{m}$ . **b2** An image from the glomerular capillary lumina. The GBM of the glomerular capillary lumina was almost covered by basement membrane material, and holes were still only partially open. Scale bar, 2.5  $\mu\text{m}$ . **c** Third renal biopsy. **c1** An image from the epithelial side of the GBM. Thickening of the basement membrane was still present. Vacuolation was present in potential spaces where the deposits might have been. The holes on the epithelium side shown in **a1** were hardly observed. Scale bar, 2.5  $\mu\text{m}$ . **c2** An image from the glomerular capillary lumina. In contrast to **c1**, openings were present on the glomerular basement membrane inward toward the glomerular capillary lumina (blue arrowheads). Electron-lucent-like areas probably represented resorption of prior subepithelial immune complexes. Scale bar, 5  $\mu\text{m}$ . GBM, glomerular basement membrane; LV-SEM, low-vacuum scanning electron microscopy.

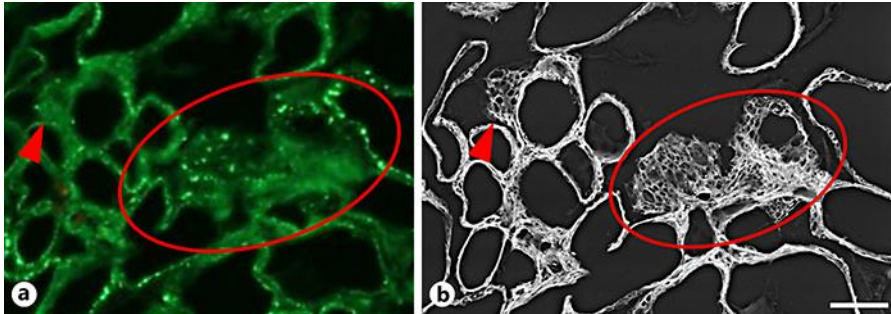


**Fig. 3.** Comparison between IF microscopy and LV-SEM findings. **a** PAM stain of an IF-stained specimen. IF staining seemed to be almost nonexistent (red arrowhead and circle). **b** LV-SEM findings did not clearly confirm the immune complex deposition in the area (red arrowhead and circle). Examination of the site with LV-SEM indicated washout of the immune complex deposition. IF, immunofluorescence; LV-SEM, low-vacuum scanning electron microscopy; PAM, periodic acid methenamine silver.

**Table 1.** Patient's laboratory results upon admission at the age of 57 years

Parameter	Value	Reference range
<i>Urine</i>		
pH	5.5	5.0–6.5
Red blood cells, /HPF	0–1	<5
Fatty casts, /WF	1–4	Negative
Epithelial casts, /WF	1–4	Negative
Urine protein/creatinine ratio, g/g	2.68	<0.15
N-acetyl- $\beta$ -D-glucosaminidase, IU/L	13.2	0.7–11.2
$\beta_2$ -Microglobulin, $\mu$ g/L	0.75	<230
<i>Blood</i>		
Leukocyte count, / $\mu$ L	4,750	4,500–9,000
Lymphocytes, / $\mu$ L	940	1,200–3,690
Hemoglobin, g/dL	11.9	13.6–17.0
Platelet count, $\times 10^4$ / $\mu$ L	20.7	14–36
Urea nitrogen, mg/dL	21.4	8.0–22.0
Creatinine, mg/dL	0.85	0.60–1.10
Estimated GFR, mL/min/1.73 m <sup>2</sup>	53	>90
Uric acid, mg/dL	6.0	3.6–7.0
Total protein, g/dL	6.2	6.7–8.3
Albumin, g/dL	3.7	4.0–5.0
Sodium, mEq/L	140	138–146
Potassium, mEq/L	5.3	3.6–4.9
Chloride, mEq/L	108	99–109
Corrected serum calcium, mg/dL	8.8	8.6–10.4
Phosphate, mg/dL	3.5	2.5–4.7
C-reactive protein, mg/dL	0.07	<0.30
CH50, CH50/mL	48.7	25–48
C3, mg/dL	98	65–135
C4, mg/dL	26	13–35
IgG, mg/dL	630	870–1,700
IgA, mg/dL	170	110–410
IgM, mg/dL	18	33–190
Anti-nuclear antibody (staining patterns)	$\times 320$ homologous, speckled	< $\times 40$
Anti-ssDNA antibody, IU/mL	2.8	<2.0
Anti-dsDNA antibody, IU/mL	5.8	<2.0

CH50, 50% hemolytic complement; dsDNA, double-stranded DNA; GFR, glomerular filtration rate; HPF, high-power field; Ig, immunoglobulin; ssDNA, single-stranded DNA; WF, whole field.